Complementing Substitutions within Loop Regions 2 and 3 of the α/β-Barrel Active Site Influence the CO_2/O_2 Specificity of Chloroplast Ribulose-1,5-bisphosphate Carboxylase/Oxygenase†

Graham Thow, Genhai Zhu, and Robert J. Spreitzer*

Department of Biochemistry, University of Nebraska, Lincoln, Nebraska 68583-0718

Received December 6, 1993; Revised Manuscript Received March 1, 1994®

ABSTRACT: An acetate-requiring mutant of the green alga *Chlamydomonas reinhardtii*, named 28-7J, has been recovered using chemical mutagenesis. It lacks ribulose-1,5-bisphosphate carboxylase/oxygenase (EC 4.1.1.39) holoenzyme, and accumulates only a small amount of the chloroplast-encoded large subunit. Pulse/chase experiments revealed that large subunits and nuclear-encoded small subunits are synthesized at normal rates. Because the mutant strain displayed uniparental inheritance and failed to complement a known chloroplast *rbc*L gene mutant strain, the 28-7J *rbc*L gene was cloned and sequenced to identify the new mutation. A single base change was found that causes large-subunit arginine-217 to be replaced by serine. This substitution occurs within α-helix 2 of the α/β-barrel active site. When photosynthesis-competent revertants were selected from mutant 28-7J, revertant R14-A was found to contain a second mutation within the *rbc*L gene. This intragenic suppressor mutation, named S14-A, causes alanine-242 to be replaced by valine within β-strand 3. Holoenzyme from the R14-A double-mutant strain was found to have a 51% reduction in the CO_2/O_2 specificity factor, primarily due to a 91% decrease in the V_{max} of carboxylation. The K_m for ribulose 1,5-bisphosphate was increased 2-fold. Although the mutant substitutions are separated by 24 residues within the primary structure, they are close to each other in the tertiary structure. In fact, the substituted residues are also close to lysine-201, which must be carbamylated and coordinated with Mg^{2+} to activate the enzyme. Although the R14-A double-mutant enzyme does not have dramatic alterations in activation, the position of the carbamylated lysyl residue within the active site may account for the difference between carboxylation and oxygenation transition-state stabilization.

Ribulose-1,5-bisphosphate (RuBP)[1] carboxylase/oxygenase (Rubisco) (EC 4.1.1.39) is a key enzyme found in all photosynthetic organisms [reviewed by Spreitzer (1993)]. It initiates photosynthetic CO_2 fixation by catalyzing the reaction between CO_2 and RuBP to produce two molecules of 3-phosphoglycerate. However, Rubisco is a bifunctional enzyme. O_2 competes with CO_2 at the same active site, resulting in a partial loss of carbon from the photosynthetic pathway. The efficiency of RuBP carboxylation relative to oxygenation is defined by the CO_2/O_2 specificity factor, $\Omega = V_cK_o/V_oK_c$ (Laing et al., 1974). Ω values have generally increased during evolutionary divergence, such that the enzyme of the eukaryotic green alga *Chlamydomonas reinhardtii* has an Ω value intermediate to those of cyanobacterial ($\Omega \approx 50$) or higher plant ($\Omega \approx 80$) enzymes (Jordan & Ogren, 1981a). However, Rubisco Ω values for several nongreen algal species may be even higher than those of higher plant enzymes (Read & Tabita, 1992). A deeper understanding of the ways in which holoenzyme structure can influence Ω may enable genetic engineering of a more efficient Rubisco.

Rubisco in plants and most prokaryotes is a hexadecamer containing equal numbers of two subunits [reviewed by Spreitzer (1993)]. In green plants, the 55-kDa large subunit is encoded by the *rbc*L chloroplast gene and the 16-kDa small subunit is encoded by a family of *rbc*S nuclear genes. The small subunit is synthesized as a precursor, which follows an ordered pathway for chloroplast uptake, processing, and assembly with large subunits in the chloroplast [reviewed by Gatenby & Ellis (1990) and de Boer & Weisbeek (1991)]. The X-ray crystal structures of spinach, tobacco, and cyanobacterial holoenzymes have been elucidated (Knight et al., 1990; Curmi et al., 1992; Newman & Gutteridge, 1993). The large subunit contains an amino terminal domain and an α/β-barrel, carboxy terminal domain. The active site is formed between the α/β-barrel domain of one large subunit and the amino terminal domain of a second large subunit (Knight et al., 1990). Large-subunit K201 also needs to be carbamylated and coordinated with Mg^{2+} to activate the enzyme (Lorimer et al., 1976; Soper et al., 1988), thereby completing the structure of the active site (Knight et al., 1990). The exact function of the small subunits within the holoenzyme is not known, but their removal from the large-subunit core causes a substantial decrease in enzyme activity (Andrews, 1988).

Two genetic strategies have been used to investigate the structure/function relationships of Rubisco. Directed mutagenesis of prokaryotic genes cloned in *Escherichia coli* has been used to make amino acid substitutions in enzymes that are subsequently purified and analyzed *in vitro*. This approach is generally aimed at assessing whether a specific residue may play an essential role in catalysis [reviewed by Hartman

† Supported by NSF Grant DCB-9005547 and published as Paper No. 10519, Journal Series, Nebraska Agricultural Research Division.

* To whom correspondence should be addressed. Phone: (402)472-2932. FAX: (402)472-7842.

® Abstract published in *Advance ACS Abstracts,* April 1, 1994.

[1] Abbreviations: RuBP, D-ribulose 1,5-bisphosphate; Rubisco, D-ribulose-1,5-bisphosphate carboxylase/oxygenase; V_c, V_{max} for carboxylation; V_o, V_{max} for oxygenation; K_c, Michaelis constant for CO_2; K_o, Michaelis constant for O_2; Ω, CO_2/O_2 specificity factor; $K_{act}(CO_2)$, activation/binding constant for CO_2; $K_{act}(Mg^{2+})$, activation/binding constant for Mg^{2+}; SDS, sodium dodecyl sulfate; PAGE, polyacrylamide gel electrophoresis; PCR, polymerase chain reaction.

0006-2960/94/0433-5109$04.50/0

(1992)]. A second strategy relies upon classical genetics [reviewed by Spreitzer (1993)]. Mutants that lack Rubisco function can be recovered by random genetic screening in the green alga *C. reinhardtii*. The responsible mutations are subsequently identified by DNA sequencing, and the deduced amino acid substitutions define an essential structural region. Because the mutations exist *in vivo*, genetic selection can then be exploited to define second-site mutations that complement the primary defect. Using this approach, amino acid interactions within the stem of large-subunit loop 6 were identified that influence Ω of Rubisco (Chen & Spreitzer, 1989; Chen et al., 1991).

Chloroplast genetic screening and selection in *C. reinhardtii* have now been used to identify a second large-subunit region that influences Ω. An acetate-requiring, photosynthesis-deficient mutant of *C. reinhardtii* has been found to arise from an *rbc*L mutation that causes an R217S substitution within the large subunit. This substitution is complemented by a second *rbc*L mutation that causes an A242V substitution 25 residues distant. The double-mutant enzyme has a reduced Ω value, which is likely to arise from altered structural interactions in the region surrounding the activator K201.

EXPERIMENTAL PROCEDURES

Strains, Culture Conditions, and Genetic Analysis. *C. reinhardtii* 2137 *mt*$^+$ was used as the wild-type strain, and the *pf-2 mt*$^-$ centromere-marker strain was used for genetic analysis (Spreitzer & Mets, 1981). All strains were maintained on solid medium containing 10 mM sodium acetate and 1.5% Select agar (Gibco/BRL) at 25 °C in darkness (Spreitzer & Mets, 1981). For biochemical analysis, cells were grown in the same medium (without agar) on a rotary shaker at 220 rpm.

Mutant Screening and Revertant Selection. Standard procedures were employed for mutant recovery (Spreitzer et al., 1992). Wild-type cells were treated with 5-fluorodeoxyuridine and mutagenized with methyl methanesulfonate in darkness (Spreitzer & Mets, 1981). Dark-grown colonies were replica plated to minimal medium to identify acetate-requiring strains. Mutant 28-7J was then recovered from a large collection of acetate-requiring mutants by employing a genetic screening procedure described previously (Spreitzer & Ogren, 1983). Spontaneous, photosynthesis-competent revertants were selected by plating mutant 28-7J cells directly on minimal medium with a light intensity of 80 μmol of photons m^{-2} s^{-1} (Chen & Spreitzer, 1989). In some reversion experiments, cells were mutagenized with methyl methanesulfonate just prior to selection (Spreitzer & Chastain, 1987). In all cases, independent clones of mutant 28-7J were used in the reversion experiments and only genetically independent revertants were retained for further analysis.

Gel Electrophoresis and Immunoblotting. Total soluble cell proteins were extracted from *C. reinhardtii* cells by sonication as described previously (Spreitzer & Chastain, 1987). Protein was quantified by the method of Bradford (1976). Nonequilibrium pH-gradient electrophoresis was performed as described by O'Farrell et al. (1977), and protein bands were visualized with bromophenol blue and Coomassie blue (Spreitzer & Mets, 1980). SDS–PAGE was performed according to the method of Laemmli (1970) by employing a 7.5–15% polyacrylamide gradient in the running gel. Proteins were then stained with Coomassie blue. Proteins separated by SDS–PAGE were blotted to nitrocellulose using a Trans-Blot apparatus (Bio-Rad) according to the method of Towbin et al. (1979). Membranes were probed with rabbit antitobacco Rubisco immunoglobulin G (5 μg mL^{-1}) provided by Dr. Raymond Chollet (Department of Biochemistry, University of Nebraska, Lincoln, NE). Goat antirabbit immunoglobulin G conjugated to horseradish peroxidase (Bio-Rad) was used as the secondary antibody. Complexes were detected using enhanced chemiluminescence (Amersham).

Pulse Labeling and Fluorography. Dark-grown, sulfate-starved cells were pulse labeled with carrier-free $H_2{}^{35}SO_4$ for 1 min and chased with 10 mM Na_2SO_4 for 60 min (Spreitzer et al., 1985). The cells were then washed, resuspended in 50 μL of 4% SDS, 20% glycerol, 10% 2-mercaptoethanol, 0.002% bromophenol blue, and 12.5 mM Tris (pH 6.8), and boiled for 5 min. Labeled proteins were separated by SDS–PAGE as described above. The gels were then treated with En^3-Hance (DuPont/NEN), dried at 60 °C, and exposed to X-ray film at −70 °C.

PCR, Gene Cloning, and DNA Sequencing. Cell pellets, containing about 2 × 10^9 cells, were resuspended in 4 mL of 100 mM NaCl, 50 mM EDTA, 1.25 mg mL^{-1} proteinase K, 1% SDS, and 20 mM Tris (pH 8.0) and incubated at 50 °C for 2 h. Nucleic acids were extracted from the lysed cells with phenol/chloroform according to standard procedures (Sambrook et al., 1989). DNA (300 ng) was digested with *Hae*III or *Eco*RI prior to initiating PCR reactions. Using oligonucleotide primers (DNA Synthesis Core Facility, University of Nebraska) complementary to the known *rbc*L sequence (Dron et al., 1982), the complete *rbc*L coding sequence was amplified (Saiki et al., 1988). The 1917-bp product was digested with *Sau*3A, and the resultant 1700-bp subfragment was isolated from a low-melting-point agarose gel (FMC BioProducts). The *Sau*3A fragment was ligated into *Bam*HI-digested pUC19 (Yanisch-Perron et al., 1985), which was then transformed into *E. coli* DH5α (Gibco/BRL). Transformants were selected and screened using standard methods (Sambrook et al., 1989). To isolate the *rbc*L gene directly from chloroplast DNA, total cellular DNA was digested with *Eco*RI and fractionated on an agarose gel. Because *rbc*L resides on a 5.6-kb *Eco*RI fragment (Dron et al., 1982), fragments of this size were cut from the gel and ligated into *Eco*RI-digested pUC19. *E. coli* transformants that contained *rbc*L plasmids were identified by analyzing restriction-enzyme digestion patterns of plasmid minipreparations prepared by the alkaline-lysis procedure (Sambrook et al., 1989). Double-stranded DNA was sequenced according to the dideoxy chain-termination method (Sanger et al., 1977) by employing various synthetic oligonucleotides, Sequenase (U. S. Biochemical Corp.), and [α-^{35}S]dATP (Amersham).

Enzyme Biochemistry and Kinetic Analysis. Preparation of crude cell extracts and further purification of Rubisco by sucrose density gradient centrifugation were performed as described previously (Spreitzer & Chastain, 1987). RuBP carboxylase activity was routinely assayed by measuring the incorporation of $^{14}CO_2$ from $NaH^{14}CO_3$ into acid-stable products (Spreitzer & Chastain, 1987). Ω was determined at 25 °C by measuring carboxylation and oxygenation simultaneously in 30-min reactions containing 10 μg of purified enzyme in 55 μM [1-^{3}H]RuBP (8.6 Ci mol^{-1}), 2 mM $NaH^{14}CO_3$ (5.0 Ci mol^{-1}), 10 mM $MgCl_2$, and 50 mM Bicine (pH 8.3) (Spreitzer et al., 1982; Jordan & Ogren, 1981b). Due to the low activity of revertant R14-A enzyme, 100 μg was used in the reactions. Other kinetic constants were determined as described previously (Chen et al., 1988; Chen & Spreitzer, 1989, 1991). To measure $K_{act}(CO_2)$, 10 or 100 μg of decarbamylated enzyme was preincubated with 500 μL of 1.56–15.56 mM $NaH^{14}CO_3$ (5 Ci mol^{-1}), 10 mM $MgCl_2$, 1

mM DTT, and 50 mM Bicine (pH 8.3) for 30 min at 25 °C. RuBP carboxylase assays were then initiated by adjusting to 5 mM $NaH^{14}CO_3$ and adding 0.5 mM RuBP to final concentrations. The reactions were terminated after 1 min with 500 μl of 1 N HCl and the solutions evaporated to dryness. Acid-stable dpm were determined by liquid scintillation spectrometry. Activation CO_2 concentrations were calculated as described by Yokota & Kitaoka (1985). To determine $K_{act}(Mg^{2+})$, 10 or 100 μg of decarbamylated enzyme was preincubated in 500 μL of 1–16 mM $MgCl_2$, 10 mM $NaH^{14}CO_3$ (5 Ci mol^{-1}), 1 mM DTT, and 50 mM Tris (pH 8.0) for 30 min at 25 °C. RuBP carboxylase assays were then initiated with 0.5 mM RuBP and terminated after 1 min. The pH dependence of carbamylation was determined by preincubating decarbamylated enzyme for 30 min at 25 °C in 10 μM CO_2, 10 mM $MgCl_2$, 1 mM DTT, 4 μg mL^{-1} carbonic anhydrase, and 0.1 M buffer (Mes, pH 6.46; Mops, pH 6.97 and 7.27; Hepes, pH 7.6 and 7.83; Tricine, pH 8.11; Bicine, pH 8.47 and 9.01). Various concentrations of $NaHCO_3$ were used to produce 10 μM CO_2 at the different pH levels, based upon the pK values of Yokota & Kitaoka (1985). RuBP carboxylase assays were initiated by adding 5 μg of wild-type or 50 μg of R14-A enzyme in preincubation solution to reaction vials at a final concentration of 1 mM $NaH^{14}CO_3$ (10 Ci mol^{-1}), 0.5 mM RuBP, 10 mM $MgCl_2$, 1 mM DTT, and 0.1 M Hepes (pH 8.0). The reactions were terminated after 1 min. Enzyme activities were normalized to a single CO_2 concentration by employing the formula of Lorimer et al. (1976).

RESULTS

Genotype and Phenotype of Mutant 28-7J. Because the 28-7J acetate-requiring mutant was recovered due its inability to recombine or complement with a defined *rbc*L mutation (mutant 10-6C *mt*⁻; Spreitzer & Mets, 1980), it was likely that the 28-7J mutant also arose from a mutation in the *rbc*L structural gene. Genetic analysis further showed that the mutant phenotype was inherited in a uniparental pattern, which is expected for a mutation within the chloroplast genome (Spreitzer et al., 1992). When the complete 28-7J *rbc*L gene was cloned and sequenced, only a single C-to-A transversion was found. This base change would cause an R217S substitution (CGU → AGU) within the Rubisco large subunit.

Crude extracts of mutant 28-7J were found to lack RuBP carboxylase activity, and no holoenzyme was detected when the extracts were fractionated on sucrose density gradients. SDS–PAGE also revealed that the mutant strain lacked both the large and small subunits of Rubisco (Figure 1, panel A). However, immunoblotting indicated that the 28-7J mutant accumulates a small amount of large subunit in the absence of small subunits (Figure 1, panel B). When 28-7J mutant cells were pulse labeled with $^{35}SO_4^{2-}$ for 5 min, small subunits were detected but not large subunits (Thow & Spreitzer, 1992). When the mutant cells were pulse labeled for only 1 min, synthesis of both large and small subunits was then observed (Figure 2, lane 2). Both subunits were subsequently degraded during a 1-h chase, but small subunit degradation appeared to be more extensive than that of the large subunit (Figure 2, lane 4). It is apparent that the R217S large-subunit substitution in mutant 28-7J affects an early step in the assembly of Rubisco holoenzyme.

Recovery of Revertants. Photosynthesis-competent revertants of 28-7J were selected by plating mutant cells on minimal medium in the light. Revertant colonies arose spontaneously at a frequency of about $1/10^8$ cells. Following methyl

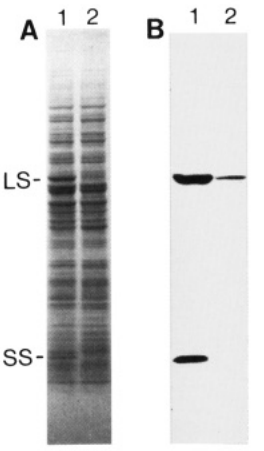

FIGURE 1: SDS–PAGE and Western analysis of total soluble proteins from wild type and mutant 28-7J (R217S). Cells were grown in the dark at 25 °C prior to extraction. Each lane received 50 μg of protein, and the gel was either stained with Coomassie blue after electrophoresis (panel A) or blotted to a filter and probed with rabbit antitobacco Rubisco immunoglobulin G (panel B). Lane 1, wild type; lane 2, mutant 28–7J. The 55-kDa large subunit (LS) and 16-kDa small subunit (SS) are indicated.

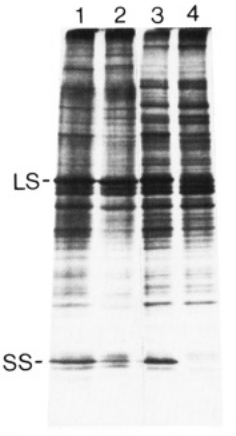

FIGURE 2: Pulse labeling of soluble cell proteins in wild type and mutant 28-7J (R217S). Dark-grown cells were labeled with $^{35}SO_4^{2-}$ for 1 min (lanes 1 and 2) and chased with 10 mM Na_2SO_4 for 1 h (lanes 3 and 4). Samples were extracted, and equal amounts of radioactivity were subjected to SDS–PAGE followed by fluorography. Lanes 1 and 3, wild type; lanes 2 and 4, mutant 28-7J. The large subunit (LS) and small subunit (SS) are indicated.

methanesulfonate mutagenesis of the 28-7J cells, revertants were found at an increased frequency of about $5/10^8$ cells. Ten genetically independent revertants were saved for further analysis. Revertants R14-A, R20-3A, R41-9A, R101-15B, and R101-18 were recovered spontaneously, and revertants R34-5A, R36-4B, R77-13, R85-16, and R92-10 were recovered after mutagen treatment. The *rbc*L gene was PCR amplified from each of the revertants and sequenced through the original mutant site. Seven of the revertants were found to result from true reversion, thereby confirming the assignment of the original 28-7J *rbc*L mutation. Two revertants, R36-4B and R41-9A, still contained the original 28-7J mutation within the *rbc*L genes. These revertants were also genetically unstable, giving rise to acetate-requiring cells when cultured with acetate medium in darkness. This form of genetic instability, referred to as heteroplasmicity (Spreitzer et al., 1984), is likely to arise from tRNA-mediated informational suppression within the chloroplast (Yu & Spreitzer, 1992). The remaining revertant, named R14-A, was particularly interesting with respect to the biochemistry of Rubisco. Its *rbc*L gene still contained the original 28-7J

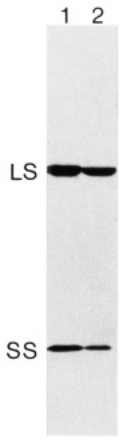

FIGURE 3: Western analysis of total soluble proteins from wild type and revertant R14-A (R217S/A242V). Cells were grown in acetate medium in the light prior to extraction. Each lane of an SDS–polyacrylamide gel received 50 μg of protein. After electrophoresis, the gel was blotted to a filter and probed with rabbit antitobacco Rubisco immunoglobulin G. Lane 1, wild type; lane 2, revertant R14–A. The large subunit (LS) and small subunit (SS) are indicated.

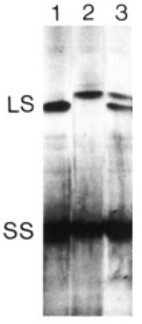

FIGURE 4: Nonequilibrium pH-gradient electrophoresis of purified Rubisco from wild type and revertant R14-A (R217S/A242V). About 6 μg of holoenzyme was subjected to denaturing electrophoresis in ampholyte-containing tube gels. The gels were subsequently stained with bromophenol blue and Coomassie blue and photographed with basic ends oriented to the bottom of the figure. Lane 1, wild type; lane 2, revertant R14-A; lane 3, mixture of wild type and R14-A. The large subunit (LS) and small subunit (SS) are indicated.

mutation, but an additional C-to-T transition mutation was also found. This second-site, intragenic suppressor mutation, named S14-A, causes an A242V amino acid substitution (GCU → GUU) 25 residues distant from the original R217S mutant substitution. To confirm that the S14-A second-site mutation was not an artifact of PCR amplification, the *Eco*RI fragment that contains *rbc*L was cloned from genomic DNA. Only the expected base changes were found when the revertant R14-A *rbc*L gene was completely sequenced.

Biochemical Analysis of Revertant R14-A. Following growth with acetate in the light (50 μmol of photons m^{-2} s^{-1}) crude extracts of revertant R14-A had about 10% of the wild-type level of RuBP carboxylase activity and, when fractionated on sucrose gradients, about 25% of the wild-type level of holoenzyme. Western analysis of the revertant cell extract further indicated that the levels of large and small subunits were reduced *in vivo* (Figure 3). When purified Rubisco was subjected to nonequilibrium pH-gradient electrophoresis (Figure 4), revertant R14-A large subunits displayed a loss of positive charge, which would be consistent with the assignment of the original R217S substitution.

Kinetic analysis of purified Rubisco revealed significant differences between the R14-A and wild-type enzymes (Table 1). The Ω value of the wild-type enzyme was 67 ± 2, but the Ω value for the R14-A (R217S/A242V) enzyme was reduced to 33 ± 1. K_o/K_c for the mutant enzyme was increased by 31%, but V_c/V_o was decreased by 63%. Thus, the 51% decrease in Ω of the R14-A enzyme arises primarily from a 91% decrease in V_c (Table 1).

Table 1: Kinetic Properties of Rubisco Purified from Wild Type and Revertant R14-A[a]

kinetic constant	wild type	R14-A (R217S/A242V)
$\Omega = V_cK_o/V_oK_c$[b]	67 ± 2	33 ± 1
K_c (μM, CO_2)	31 ± 3	235 ± 15
K_o (μM, O_2)	397 ± 21	4032 ± 59
V_c [μmol h^{-1} (mg of protein)$^{-1}$]	122 ± 7	11 ± 2
K_o/K_c[c]	13	17
V_c/V_o[c]	5.2	1.9
K_m (μM, RuBP)	18 ± 2	41 ± 5

[a] The values are the means of three separate enzyme preparations with sample ($n-1$) standard deviations. [b] V_cK_o/V_oK_c is the CO_2/O_2 specificity factor (Jordan & Ogren, 1981b; Laing et al., 1974). [c] Calculated values.

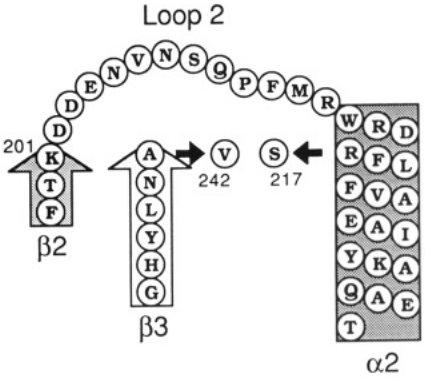

FIGURE 5: Amino acid substitutions within loop regions 2 and 3 of the α/β-barrel active site of *C. reinhardtii* Rubisco. The arginine-217-to-serine substitution (R217S), caused by the 28-7J mutation, can be complemented by the alanine-242-to-valine (A242V) substitution, caused by the S14-A mutation. The activator lysyl residue occurs at amino acid position 201 (Soper et al., 1988). The locations of the β-strands (vertical arrows) and the α-helix (vertical box) are based on the crystal structure of spinach Rubisco (Knight et al., 1990).

The original 28-7J (R217S) mutant substitution occurs in α-helix 2 of the α/β-barrel, and the complementing S14-A (A242V) substitution occurs within β-strand 3 (Figure 5). On the basis of the X-ray crystal structure of spinach Rubisco, it is known that the side chains of R217 and A242 are within the hydrophobic environment that exists between the α-helixes and β-strands of the α/β-barrel wall (Knight et al., 1990). Because R217 forms an ionic bond with D202 (Knight et al., 1990), it seemed reasonable to consider that the mutant substitutions in the R14-A (R217S/A242V) enzyme might influence the activator K201 (Figure 5). When activator CO_2 and Mg^{2+} binding were investigated, only slight differences were found between purified R14-A and wild-type enzymes. Wild-type enzyme had a $K_{act}(CO_2)$ of 13 μM and a K_{act}-(Mg^{2+}) of 1.8 mM, and the R14-A revertant enzyme had values of 16 μM and 2.4 mM, respectively. Furthermore, by using the method described by Lorimer et al. (1976), the apparent pK of the activator K201 was estimated for the mutant and wild-type enzymes by measuring carbamylation state at various pH levels. Once again, no substantial difference was observed. The apparent pK for the wild-type enzyme was found to be 7.42, and that of the R14-A mutant enzyme was 7.67.

DISCUSSION

The 28-7J mutant was identified by screening for acetate-requiring, RuBP-carboxylase-deficient mutants of *C. rein-*

hardtii. Although the mutant strain can synthesize both large and small subunits of Rubisco (Figure 2), these subunits fail to accumulate to any significant extent (Figure 1) and no holoenzyme can be isolated. This deficiency in holoenzyme assembly results from a chloroplast *rbc*L gene mutation that causes an R217S substitution within the Rubisco large subunit. On the basis of the X-ray crystal structure of the spinach enzyme (Knight et al., 1990), R217 is located within α-helix 2 of the α/β-barrel active site. It forms an ionic bond with D202 (Figure 5), allowing the side chains of both residues to be buried within the hydrophobic environment between the α-helixes and β-strands of the barrel wall (Knight et al., 1990). The R217S substitution caused by the 28-7J mutation would disrupt the ionic interaction with D202, which may then account for a disorganization of large-subunit folding. A number of residues in α-helix 2 also interact with small subunits (Figure 5; Knight et al., 1990). Small-subunit residues form ionic bonds with K227 and E223 and pack against a large-subunit hydrophobic surface defined in part by L219, A222, and Y226. The R217S substitution might also disrupt such intersubunit interactions. Whatever the case, it is clear that the R217S substitution destabilizes holoenzyme assembly, leading to the degradation of Rubisco subunits *in vivo* (Figure 1).

As a means for further investigating the structural significance of the R217S substitution, photosynthesis-competent revertants were selected from the 28-7J mutant strain. Of 10 genetically independent revertants analyzed, only one arose from a second-site mutation within the Rubisco structural genes. This revertant strain, named R14-A, contains an additional *rbc*L mutation, named S14-A, that causes an A242V substitution within the large subunit (Figure 5). The fact that only one form of intragenic suppression was identified indicates that there are very few ways to structurally complement the original R217S substitution. Furthermore, because the specific S14-A mutation was not recovered more than once, one could assume that R14-A (R217S/A242V) Rubisco still had deficiencies that reduced the chance of selecting a revertant cell, based upon photosynthetic ability. Such an assumption proved to be warranted. The R14-A holoenzyme fails to accumulate to the wild-type level (Figure 3), and the purified enzyme has a 51% decrease in Ω due to a 63% decrease in V_c/V_o (Table 1).

The S14-A A242V substitution occurs in β-strand 3, 25 residues away from the primary R217S substitution in α-helix 2 (Figure 5). A242, like R217 and D202, is located within the hydrophobic environment that is formed between α-helixes and β-strands of the α/β-barrel active site (Knight et al., 1990). A destabilizing cavity created by replacing R217 with a substantially smaller seryl residue might then be partially filled by replacing A242 with the larger valyl residue. The exact nature of the amino acid interactions responsible for eliminating or restoring holoenzyme assembly will require future application of directed mutagenesis and X-ray crystallography.

It is interesting that the R14-A (R217S/A242V) enzyme has a reduced Ω value (Table 1). Ω is determined by the differential stabilization of the carboxylation and oxygenation transition states for the partial reactions between the 2,3-enediolate of RuBP and the CO_2 and O_2 gaseous substrates (Pierce et al., 1986; Chen & Spreitzer, 1991, 1992). Activator Mg^{2+}, coordinated to carbamylated K201, is likely to be involved in stabilizing these transition states (Knight et al., 1990; Chen & Spreitzer, 1992). This is most apparent from the fact that replacement of Mg^{2+} with Mn^{2+} causes a marked decrease in the value of Ω (Jordan & Ogren, 1981b). Perhaps the R217S and A242V amino acid substitutions in the R14-A enzyme influence Ω by affecting the position or chemical environment of the activator Mg^{2+}. Clearly, the R217S substitution disrupts the ionic interaction between R217 and D202, and the complementing A242V substitution restores *in vivo* holoenzyme stability only partially. The persisting changes in structure may influence the neighboring activator K201 or change the positions of the D203 or E204 side chains that also serve as ligands for the metal ion (Knight et al., 1990). Although significant changes were not found when the R14-A (R217S/A242V) enzyme was analyzed with respect to $K_{act}(CO_2)$, $K_{act}(Mg^{2+})$, or the apparent pK for the activator lysyl residue, subtle changes in structure may have dramatic effects on Ω. Using the Ω values in Table 1, one can calculate the difference between the energies of activation for the oxygenation and carboxylation partial reactions ($\Delta G_o^{\ddagger} - \Delta G_c^{\ddagger}$) (Chen & Spreitzer, 1991, 1992). These values are 10.42 kJ mol^{-1} for the wild-type enzyme and 8.67 kJ mol^{-1} for the R14-A double-mutant enzyme. Thus, a relatively small kinetic change of only 2 kJ mol^{-1} can account for a 51% decrease in Ω (Table 1).

Directed mutagenesis has been used to investigate a number of residues flanking the activator lysyl residue of the homodimeric, large-subunit-like holoenzyme of the photosynthetic bacterium *Rhodospirillum rubrum*. Substitutions at residues homologous to K201, D203, and E204 (Figure 5) eliminated activity of the purified enzyme (Estelle et al., 1985; Gutteridge et al., 1988), and X-ray crystallography of the D203N mutant enzyme revealed extensive alterations in structure (Söderlind et al., 1992), further indicating a close connection between large-subunit folding and catalysis in this region. However, conservative changes at positions homologous to large-subunit residues 198, 200, and 202 had little or no effect (Gutteridge et al., 1984, 1988). An N202D substitution, designed to make the *R. rubrum* enzyme more like the chloroplast enzyme (Figure 5), caused less than a 50% decrease in RuBP carboxylase activity with no apparent change in Ω (Gutteridge et al., 1988). Considering that the homodimeric *R. rubrum* enzyme normally has N202 and T217 (Nargang et al., 1984), instead of the D202 and R217 salt-linked residues of the chloroplast enzyme (Knight et al., 1990), one might expect that the bacterial enzyme would have structure–function relationships that are different from the eukaryotic enzyme. It is also interesting that the *R. rubrum* enzyme has a bulky isoleucyl residue in place of the A242 residue normally present in chloroplast enzymes (Knight et al., 1990). In contrast, the plant-like Rubisco of the cyanobacterium *Anacystis nidulans* has residues homologous to D202 and R217 of chloroplast enzymes, but it has a valyl residue in place of A242 (Shinozaki et al., 1983). In the present study, an A242V substitution has been found to complement an R217S substitution in the chloroplast enzyme (Figure 5), and these substitutions cause a reduction in the value of Ω (Table 1). It would be interesting to determine the effect of an R217S or V242A substitution on the cyanobacterial enzyme. Further investigation of tertiary structure interactions in the loop 2/loop 3 region may provide deeper insight into the structural basis of catalytic efficiency.

ACKNOWLEDGMENT

We thank Sam Spilker for technical assistance and Antonin Gauthier, Donghong Zhang, and Shan Sivakumaran for recovering several of the revertant strains. Zhixiang Chen

and Donghong Zhang also contributed to the early phases of mutant and revertant analysis.

REFERENCES

Andrews, T. J. (1988) *J. Biol. Chem. 263*, 12213–12219.

Bradford, M. (1976) *Anal. Biochem. 72*, 248–254.

Chen, Z., & Spreitzer, R. J. (1989) *J. Biol. Chem. 264*, 3051–3053.

Chen, Z., & Spreitzer, R. J. (1991) *Planta 183*, 597–603.

Chen, Z., & Spreitzer, R. J. (1992) *Photosynth. Res. 31*, 157–164.

Chen, Z., Chastain, C. J., Al-Abed, S. R., Chollet, R., & Spreitzer, R. J. (1988) *Proc. Natl. Acad. Sci. U.S.A. 85*, 4696–4699.

Chen, Z., Yu, W., Lee, J. H., Diao, R., & Spreitzer, R. J. (1991) *Biochemistry 30*, 8846–8850.

Curmi, M. G., Cascio, D., Sweet, R. M., Eisenberg, D., & Schreuder, H. (1992) *J. Biol. Chem. 267*, 16980–16989.

de Boer, A. D., & Weisbeek, J. J. (1991) *Biochim. Biophys. Acta 1071*, 221–253.

Dron, M., Rahiré, M., & Rochaix, J. D. (1982) *J. Mol. Biol. 162*, 775–793.

Estelle, M., Hanks, J., McIntosh, L., & Somerville, C. (1985) *J. Biol. Chem. 260*, 9523–9526.

Gatenby, A. A., & Ellis, R. J. (1990) *Annu. Rev. Cell. Biol. 6*, 125–149.

Gutteridge, S., Sigal, I., Thomas, B., Arentzen, R., Cordova, A., & Lorimer, G. (1984) *EMBO J. 3*, 2737–2743.

Gutteridge, S., Lorimer, G., & Pierce, J. (1988) *Plant Physiol. Biochem. 26*, 675–682.

Hartman, F. C. (1992) in *Plant Protein Engineering* (Shewry, P. R., & Gutteridge, S., Eds.) pp 61–92, Cambridge University Press, Cambridge.

Jordan, D. B., & Ogren, W. L. (1981a) *Nature 291*, 513–515.

Jordan, D. B., & Ogren, W. L. (1981b) *Plant Physiol. 67*, 237–245.

Knight, S., Andersson, I., & Brändén, C. I. (1990) *J. Mol. Biol. 215*, 113–160.

Laemmli, U. K. (1970) *Nature 227*, 680–685.

Laing, W. A., Ogren, W. L., & Hageman, R. H. (1974) *Plant Physiol. 54*, 678–685.

Lorimer, G. H., Badger, M. R., & Andrews, T. J. (1976) *Biochemistry 15*, 529–536.

Nargang, F., McIntosh, L., & Somerville, C. (1984) *MGG, Mol. Gen. Genet. 193*, 220–224.

Newman, J., & Gutteridge, S. (1993) *J. Biol. Chem. 268*, 25876–25886.

O'Farrell, P. Z., Goodman, H. M., & O'Farrell, P. H. (1977) *Cell 12*, 1133–1142.

Pierce, J., Andrews, T. J., & Lorimer, G. H. (1986) *J. Biol. Chem. 261*, 10248–10256.

Read, B. A., & Tabita, F. R. (1992) *Biochemistry 31*, 5553–5559.

Saiki, R. K., Gelfand, D. H., Stoffel, S., Scharf, S. J., Higuchi, R., Horn, G. T., Mullis, K. B., & Erlich, H. A. (1988) *Science 239*, 487–491.

Sambrook, J., Fritsch, E. F., & Maniatis, T. (1989) *Molecular Cloning: A Laboratory Manual*, Cold Spring Harbor Laboratory, Cold Spring Harbor.

Sanger, F., Nicklen, S., & Coulsen, A. R. (1977) *Proc. Natl. Acad. Sci. U.S.A. 74*, 5463–5467.

Shinozaki, K. Yamada, C., Takahata, N., & Sugiura, M. (1983) *Proc. Natl. Acad. Sci. U.S.A. 80*, 4050–4054.

Söderlind, E., Schneider, G., & Gutteridge, S. (1992) *Eur. J. Biochem. 206*, 729–735.

Soper, T. S., Mural, R. J., Larimer, F. W., Lee, E. H., Machanoff, R., & Hartman, F. C. (1988) *Protein Eng. 2*, 39–44.

Spreitzer, R. J. (1993) *Annu. Rev. Plant Physiol. Plant Mol. Biol. 44*, 411–434.

Spreitzer, R. J., & Chastain, C. J. (1987) *Curr. Genet. 11*, 611–616.

Spreitzer, R. J., & Mets, L. (1980) *Nature 285*, 114–115.

Spreitzer, R. J., & Mets, L. (1981) *Plant Physiol. 67*, 565–569.

Spreitzer, R. J., & Ogren, W. L. (1983) *Proc. Natl. Acad. Sci. U.S.A. 80*, 6293–6297.

Spreitzer, R. J., Jordan, D. B., & Ogren, W. L. (1982) *FEBS Lett. 148*, 117–121.

Spreitzer, R. J., Chastain, C. J., & Ogren, W. L. (1984) *Curr. Genet. 9*, 83–89.

Spreitzer, R. J., Goldschmidt-Clermont, M., Rahiré, M., & Rochaix, J. D. (1985) *Proc. Natl. Acad. Sci. U.S.A. 82*, 5460–5464.

Spreitzer, R. J., Thow, G., Zhu, G., Chen, Z., Gotor, C., Zhang, D., & Hong, S. (1992) in *Research in Photosynthesis* (Murata, N., Ed.) Vol. III, pp 593–600, Kluwer Academic Publishers, Dordrecht.

Thow, G., & Spreitzer, R. J. (1992) in *Research in Photosynthesis* (Murata, N., Ed.) Vol. III, pp 633–636, Kluwer Academic Publishers, Dordrecht.

Towbin, H., Staehelin, T., & Gordon, J. (1979) *Proc. Natl. Acad. Sci. U.S.A. 76*, 4350–4354.

Yanisch-Perron, C., Vieira, J., & Messing, J. (1985) *Gene 33*, 103–119.

Yokota, A., & Kitaoka, S. (1985) *Biochem. Biophys. Res. Commun. 131*, 1075–1079.

Yu, W., & Spreitzer, R. J. (1992) *Proc. Natl. Acad. Sci. U.S.A. 89*, 3904–3907.